

The primary factors controlling the state of physico-chemical equilibrium of natural aqueous solutions are the oxidation-reduction potential (Eh) and the pH. The most sensitive to changes in the pH and Eh conditions of the solution are iron compounds, and for that reason they usually make up the body of sediments encrusting well screens. According to Hem (1961), Garrels and Christ (1965) and Barnes and Clarke (1969), it is possible to calculate the equilibrium state of an aqueous solution and determine the tendency of well-encrusting sediments to precipitate. To do this, it is essential to have a knowledge not only of the Eh and pH conditions and the general composition of an aqueous solution but also of the nature and properties of the sediment that constitutes the solid phase taking part in the reaction.

The present work aimed to analyse the mineralogical composition of sediments precipitating in wells and, specifically, to explain the nature and structure of the constituent iron compounds. Accordingly, chemical, thermal, X-ray, infrared spectroscopic and electron microscope investigations were carried out on an averaged sample of sediments encrusting one of the well screens in the area of Kraków. Three other samples collected from different parts of that screen were subjected to Mössbauer spectroscopic analyses.

## DETERMINATION OF THE MINERALOGICAL COMPOSITION OF THE SEDIMENTS

### Experimental

Quantitative chemical analysis of the sediments in question was performed in the full range according to the principles of classical gravimetric analysis of silicates. Moreover, to determine iron content, the sample was dissolved in HCl and HF solution and quantitative determinations were made in a Pye Unicam SP-90 atomic absorption spectrophotometer. The  $\text{Fe}^{2+}$  content was found by titration with  $\text{KMnO}_4$  in an atmosphere of nitrogen whereas that of  $\text{SO}_3$  by gravimetric analysis, using  $\text{BaCl}_2$ . The amount of amorphous  $\text{SiO}_2$  and  $\text{Al}_2\text{O}_3$  was also determined, employing colorimetry with ammonium molybdate for the former compound and complexometry with disodium versenate for the latter. The organic substance in the sediments studied was identified by Tiurin's method (1951). It was extracted from the sediments with a 1:1 mixture of benzene and ethyl alcohol in Soxhlet apparatus. The resultant solution was evaporated, the remainder serving as a basis for determinations of the composition of the organic substance.

X-ray diffraction analysis was carried out in a TUR M-61 apparatus in an angle range of  $4 - 65^\circ \Theta$ , using filtered  $\text{CoK}_{\alpha}$  radiation.

Thermal analysis was made in the F. Paulik, J. Paulik, L. Erdey derivatograph.

Infrared absorption spectra were recorded in the UR-10 (C. Zeiss) spectrophotometer in the range of wave numbers  $400 - 1800 \text{ cm}^{-1}$  and  $3200 - 3600 \text{ cm}^{-1}$ , using KBr disks (1.5 mg of the substance and 300 mg KBr).

Tadeusz RATAJCZAK \*, Stanisław WITCZAK \*\*, Dominik S. KULGAW-CZUK \*\*\*, Janusz KRACZKA \*\*\*

## STUDIES OF THE NATURE OF IRON COMPOUNDS IN WELL-ENCRUSTING SEDIMENTS

UKD 549.517.2.01 + 549.521.51.01 : 552.56 : 628.112.2 (438.311)

**A b s t r a c t.** Chemical and thermal analyses, electron microscopy, X-ray diffractometry, as well as IR spectroscopy and Mössbauer spectroscopy were employed to investigate the composition and structure of well-encrusting sediments. Special attention was paid to iron compounds, which make up the body of the sediments, appearing as goethite, hydrated haematite, hydrated goethite and siderite. Gel  $\text{Fe(OH)}_3$  may also be present in the sediments. It has been found that the content of iron mineral compounds (in wt. %) is:  $\alpha - \text{FeOOH} - 27 - 29$ ,  $\alpha - \text{FeOOH} \cdot n\text{H}_2\text{O} -$  about 18,  $\alpha - \text{Fe}_2\text{O}_3 \cdot n\text{H}_2\text{O} - 44$ ,  $\text{FeCO}_3 - 8 - 12$ . Iron minerals appear in fine-dispersive forms showing disarranged internal structure. For goethite, the size of crystallites was calculated, and the following results obtained: length  $100 - 500 \text{ \AA}$ , thickness about  $19 \text{ \AA}$ , dimension in the direction perpendicular to  $(110)$  plane — about  $39 \text{ \AA}$ .

### INTRODUCTION

A loss of physico-chemical equilibrium in the aqueous solution during well exploitation of waters results in the precipitation of chemical substances on the screen, pump and pipelines carrying the water away. This process, defined as incrustation, shortens considerably the life of wells which are productive, as a rule, from 2 to 6 years in shallow aquifers. The knowledge of the whole process of incrustation as well as of the composition of sediments forming on screens is of great practical significance since it serves as a basis for studies aiming to prolong the lives of wells.

\* Academy of Mining and Metallurgy, Institute of Geology and Mineral Deposits, Cracow (Kraków).

\*\* Academy of Mining and Metallurgy, Institute of Hydrogeology and Engineering Geology, Cracow (Kraków).

\*\*\* Institute of Nuclear Physics, Cracow (Kraków).

## Mineralogical composition of sediments

Chemical analyses have shown that  $\text{Fe}_2\text{O}_3$  is the dominant component of the sediments studied.  $\text{FeO}$  and  $\text{CaO}$  appear in lesser amounts while  $\text{SiO}_2$  and  $\text{Al}_2\text{O}_3$  are subordinate constituents. A high content of iron oxides in the samples ( $\text{Fe}_2\text{O}_3 + \text{FeO} = 64.05$  wt. %) qualifies the sediments as ferruginous. The full composition of the sediments is given in Table 1. It agrees well with that reported by other authors (Gawrilko 1968; Marton, Sellyey 1971; Milichiker 1971; Ratajczak, Witczak 1973; Kommunar 1974).

Table 1  
Chemical composition of investigated sediments

| Component               | Content (weight %) | Component              | Content (weight %) |
|-------------------------|--------------------|------------------------|--------------------|
| $\text{SiO}_2$          | 2.70               | $\text{K}_2\text{O}$   | 0.12               |
| $\text{TiO}_2$          | 0.35               | $\text{Na}_2\text{O}$  | 0.36               |
| $\text{Al}_2\text{O}_3$ | 1.14               | $\text{SO}_3$          | 0.65               |
| $\text{Fe}_2\text{O}_3$ | 60.10              | org. matter            | 3.10               |
| $\text{FeO}$            | 3.95               | $\text{CO}_2$          | 5.94               |
| $\text{CaO}$            | 4.05               | $\text{H}_2\text{O}^+$ | 5.07               |
| $\text{MgO}$            | 0.06               | $\text{H}_2\text{O}^-$ | 10.24              |
| $\text{MnO}$            | 0.01               | loss on ignition       | 2.12               |
| Total                   |                    |                        | 99.96              |

Amorphous compounds make up the bulk of the determined  $\text{SiO}_2$  and  $\text{Al}_2\text{O}_3$ , amounting to 81.5% (2.20 wt. %) in the case of  $\text{SiO}_2$  and to 88.6% (1.01 wt. %) in the case of  $\text{Al}_2\text{O}_3$ . Organic substance makes up 3.10 wt. % of the sediments. To identify its constituent functional groups, the concentrate obtained in Soxhlet apparatus was subjected to infrared spectroscopic analyses. These have shown that the main components of the organic substance are long-chain aliphatic hydrocarbons, also including those with polar groups having a character of esters and carboxylic acids. Generally speaking, the organic substance of the well-encrusting sediments consists of a mixture of paraffin-aliphatic hydrocarbons, which statement is consistent with the earlier results (Aleksejev 1975; Ratajczak 1976).

From X-ray investigations it appears that the well-encrusting sediments are made up predominantly of hydrated iron oxides (hydrohaematite and hydrogoethite) and hydroxides (goethite). The intensity of reflections is highly suggestive of the prevalence of hydrated iron oxides, i.e. hydrogoethite and hydrohaematite (Fig. 1). The presence of goethite is evidenced by reflections arising from the lattice planes (110) and (111), for which the  $d$  values are 4.20 and 2.46 Å respectively. An analysis of the X-ray diffractogram suggests that the sediments in question are concentrations of fine-dispersive iron oxide mineral phases showing a low degree of ordering or disarrangement of the structure. For that reason, their unequivocal identification becomes a real problem, an additional impediment being that their basal reflections show considerable coincidences. In consequence, the presence of haematite in the sediments studied is none too certain.

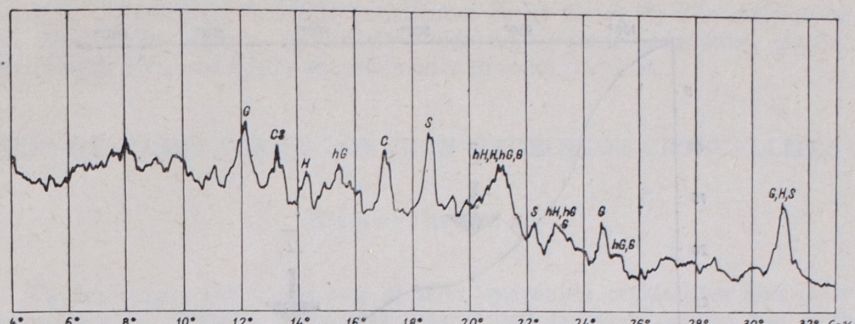


Fig. 1. X-ray powder pattern of incrustations in wells  
G — goethite,  $hG$  — hydrogoethite, H — haematite,  $hH$  — hydrohaematite, C — calcite, S — syderite

X-ray diffractometry has also revealed the presence of carbonates, calcite and siderite in the samples, which is evidenced by fairly distinct reflections from the (1012) and (1014) planes with the  $d$  values being, respectively, 3.83 and 3.02 Å for calcite and 3.59 and 2.78 Å for siderite (Fig. 1).

The dominant bands appearing in the infrared absorption spectra are due to iron oxides and hydroxides (Fig. 2). Yet, only goethite could be

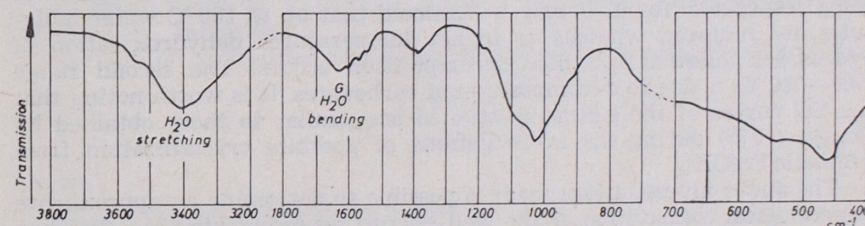


Fig. 2. IR absorption of incrustation well  
G — goethite

identified unmistakably basing on the spectra (White, Roy 1964). That the compounds in question show a high degree of hydration is evident from the bands produced by valence and deformation vibrations of  $\text{H}_2\text{O}$  molecules in the range  $3100 - 3600 \text{ cm}^{-1}$  and  $1500 - 1700 \text{ cm}^{-1}$ , respectively. A similar spectrum was obtained by Domka (1975), who investigated synthetic  $\text{Fe}(\text{OH})_3$ .

Thermal investigations have shown that TG curve is particularly useful for identification of phase composition of the sediments. DTA curve is substantially "deformed" owing to the presence of organic substance, sulphides and carbonates besides iron oxides in the analysed sample. Consequently, an unequivocal identification of those phases presents considerable difficulties due to the coincidence of thermal peaks. The temperature range of 100 — 400°C is the most diagnostic for hydrated iron oxide compounds. On the TG curve (Fig. 3), two distinct ranges of weight loss of the substance studied may be distinguished. One corresponds to the range

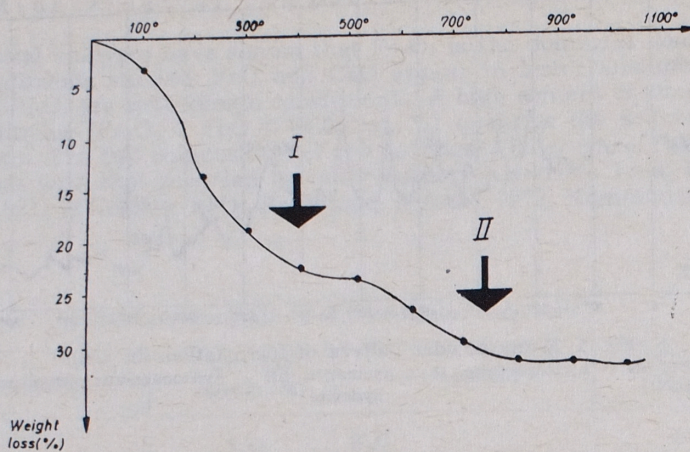


Fig. 3. Thermogravimetric curve of investigated sediments  
I — Weight loss caused by dehydration of hydrated oxides and hydroxides of Fe, by decomposition of pyrite and combustion of organic substances, II — Weight loss due to decomposition of syderite

100—400°C, the loss of water contained in the hydrated iron oxides and hydroxides as well as decomposition of organic substance and sulphates being responsible for it. It may be assumed that up to 150°C water molecules are removed whereas at higher temperatures dehydroxylation of hydroxides followed by their decomposition occurs. The second range (500—800°C) is due to decomposition of carbonates. It is worth noting that the TG curves of the sediments studied are similar to those obtained by Domka (1975) during his investigations of goethite crystallization from synthetic  $\text{Fe(OH)}_3$ .

The above investigations made it possible to determine an approximate mineralogical composition of the well-encrusting sediments (Tab. 2). They have shown that the dominant components are hydrated iron oxides of the hydrohaematite and hydrogoethite type, making up about one half of

Table 2

Approximate mineral composition of investigated sediments obtained in result of recalculations of chemical analysis and thermogravimetric curve (weight %)

| Phase                                  | Method of investigation |                         |
|--|-------------------------|-------------------------|
|  | Chemical analysis       | Thermogravimetric curve |
| $\text{SiO}_2 + \text{Al}_2\text{O}_3$ | 3.84                    | ca. 23                  |
| goethite                               | ca. 24                  |                         |
| hydrated oxides of Fe                  | 57                      | 46                      |
| org. matter                            | 3                       | 5                       |
| $\text{CaCO}_3$                        | 7                       | 9.5                     |
| $\text{FeCO}_3$                        | 6                       | 8.5                     |

the mass of samples. Goethite constitutes about 25 wt. %. The content of the other components, i.e. calcite, siderite, organic substance, pyrite, amorphous  $\text{SiO}_2$  and  $\text{Al}_2\text{O}_3$ , amounts only to some per cent.

## SIZE DETERMINATIONS FOR IRON HYDROXIDE CRYSTALLITES

### Experimental

To determine the grain size of iron hydroxide crystallites and their morphological features, appropriate investigations were carried out with the aid of a Tesla 613 BS transmission electron microscopé. The preparations were made using suspension powder technique. They were obtained from the finest fraction of the sample by dispergation in alcohol suspension. The suspension was then placed on copper grids coated with a 250 Å thick carbon film. Micrographs of the particles were taken on Agfa Gevert glass plates at magnifications of 30 000—100 000  $\times$ .

The size of iron hydroxide crystallites was also determined by X-ray method, using heated tungsten powder of grain-size of 1  $\mu$  as standard. Prior to examinations, tungsten was annealed to relieve internal stresses that cause diffusion of the diffraction lines. 10 wt. % of tungsten was added to the analysed sediment sample, and the mixture was thoroughly homogenized. For the resultant mixtures X-ray diffraction patterns were taken in the angle range of 4—65°  $\Theta$ , using a TUR M-61 diffractometer and filtered  $\text{CoK}_{\alpha}$  radiation.

The size of crystallites was calculated from Scherrer's formula (1961):

$$L_{hkl} = \frac{K \cdot \lambda \cdot R}{AB \cdot \cos \Theta}$$

where:

$L$  — average length of the crystallite (Å)

$K$  — constant (0.94)

$\lambda$  — wavelength (Å)

$R$  — camera radius (mm)

$AB$  — ( $B - B_0$ ) (mm), difference of the breadths of the line B (sample investigated) and  $B_0$  (standard sample)

$\Theta$  — glancing angle

### Results

Electron micrographs have yielded information on the structure of sediments (Phot. 1—5). The grains are usually irregular in shape (Phot. 1). Some aggregates have granular texture and well developed boundaries (Phot. 2). The grain shown on Phot. 3 has triangular outlines and sharp contours. The largest group is represented by particles with platy structure that form aggregates (Phot. 4). In one case (Phot. 5), plates with irregular, "corrugated" edges have been observed. The individual phases making up the sediment in question were identified on the basis of the atlas of Beutelspacher and Van der Marel (1968). A comparison of the micro-

graphs obtained with the standard ones has revealed their close resemblance to goethite and iron oxides. The grains are 100—500 Å in size.

Mineralogical analyses have shown that hydrated iron oxides and hydroxides are the principal components of the sediments. Diffused reflections noted in the X-ray diffraction patterns suggest that sediment crystallites are of inconsiderable size (Fig. 1). Goethite reflections are most pronounced, which is indicative of a high degree of ordering of its internal structure, and this was just one of the reasons for choosing that mineral for crystallite size determinations. The determinations were based on  $110$  and  $010$  reflections. Half-breadth of the standard reflection in the angle range comprising  $110$  and  $010$  reflections of goethite was calculated by extrapolation.

The following results were obtained:  $\perp(110) = 39.14 \text{ \AA}$ ,  $\perp(010) = 19.04 \text{ \AA}$ .

Figure 4 shows a goethite crystal acc. to Goldschmidt and Parsons (1910 — fide Mineralogy 1967) along with the values for its dimensions. The

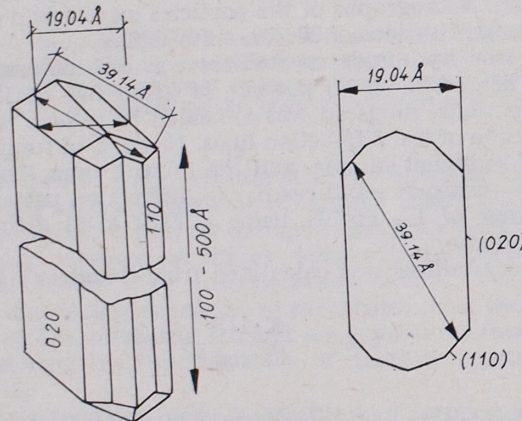


Fig. 4. Goethite crystal (after Goldschmidt and Parsons 1910) with marked  $hkl$  values

calculated size of crystallites indicates that they appear in the form of prisms, plates or rods. From electron microscope investigations it is evident that single goethite crystals are very small in size and elongated in shape. Their length varies from 100 to 500 Å, their thickness is about 19 Å, and the dimension in the direction perpendicular to  $(110)$  plane about 39 Å.

#### MÖSSBAUER SPECTROSCOPIC INVESTIGATIONS OF THE WELL-ENCRUSTING SEDIMENTS

As has been demonstrated by chemical and phase analyses, the well encrusting sediments contain mainly iron compounds. Therefore, their investigation by Mössbauer spectroscopy looked promising.

Mössbauer analyses can yield data on the Fe electron states, the nature of chemical bonding, the coordination type, the internal magnetic fields,

and on the electric field gradients that affect locally iron ions. From the intensity ratio of the respective component lines, the composition and nature of the iron compounds present in a sample may be determined.

Moreover, Mössbauer spectroscopy is sensitive to the size of crystallites. It has been shown that the nature of the magnetic and quadrupole interactions measured with the aid of Mössbauer technique for bulk materials is in several cases different than that for the same materials occurring in fine-dispersive form (crystallite size below some hundred Å). In the case of magnetically ordered (ferro- or antiferromagnetic) substances, the characteristic Zeeman splitting disappears below certain critical size limit, and only a doublet of the quadrupole splitting or a simple line may be observed in the spectrum.

An Intertechnique spectrometer operated in time mode was used to measure the Mössbauer spectra in the well-encrusting sediments. The source of the monoenergetic 14.4 keV gamma-line was  $^{57}\text{Co}$  in chromium of an activity of about 30 mCi. The absorbers were prepared from powders compressed into disks (2 cm in diameter) with a surface density of 30 mg/cm<sup>2</sup>. The spectrometer velocity scale was calibrated using the standard absorber  $a = \text{Fe}_2\text{O}_3$  enriched in the isotope  $^{57}\text{Fe}$ .

The shapes of the measured Mössbauer spectra taken at room temperature for several samples are almost identical. One of them is shown in Figure 5.

The high value of the effect as well as three clearly separated lines of different intensity imply that the measured spectra represent a superposi-

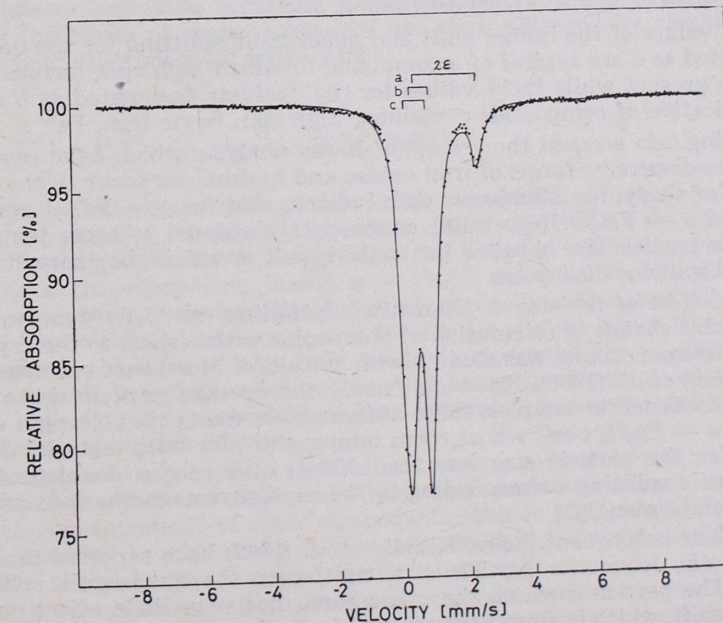


Fig. 5. Mössbauer spectrum of incrustation taken at room temperature  
 $a, b, c$  — doublets of quadrupole splitting  $2\epsilon$

tion of some doublets of the quadrupole splitting, corresponding to different sites occupied by iron ions. The spectra failed to show the Zeeman splitting, characteristic of magnetic iron compounds, which suggests that in the sample studied iron compounds appear in paramagnetic or superparamagnetic state.

Table 3

The values of quadrupole splitting  $2\epsilon$ , isomeric shift  $\delta$  and percentage of surface  $S$  for particular doublets (*a*, *b*, *c*)

| Doublet  | $2\epsilon$<br>( $\pm 0.10$ mm s $^{-1}$ ) | $\delta$<br>( $\pm 0.05$ mm s $^{-1}$ ) | $S$<br>( $\pm 2\%$ ) |
|----------|--|---|----------------------|
| <i>a</i> | 2.07                                       | 1.23                                    | 12                   |
| <i>b</i> | 0.64                                       | 0.47                                    | 46                   |
| <i>c</i> | 0.73                                       | 0.37                                    | 42                   |

A more detailed analysis of the measured spectra, carried out by an Odra-1305 computer, permitted to resolve the experimental spectra into three doublets of the quadrupole splitting having a Lorentz line shape. The fitting of the theoretical line to the experimental points is presented in Figure 5 as a solid line, whereas the position of each doublet is marked with braces *a*, *b* and *c*. The obtained values for the quadrupole splittings  $2\epsilon$ , isomer shifts  $\delta$ , as well as the surface area  $S$  under the lines for each doublet (*a*, *b*, *c*) are given in Table 3.

The values of the isomer shift and quadrupole splitting for the doublet designated as *a* are typical of a compound in which high spin ferrous iron,  $\text{Fe}^{2+}$ , is present while those values for the doublets designated as *b* and *c* are indicative of compounds containing high spin ferric iron,  $\text{Fe}^{3+}$ .

Taking into account the results of X-ray analysis which have revealed that fine-dispersive forms of iron oxides and hydroxides occur in the sample under study, the Mössbauer data indicate that for *a* —  $\text{Fe}_2\text{O}_3$  (haematite) and *a* —  $\text{FeOOH}$  (goethite), magnetically ordered at room temperature, the particle size is below the critical limit at which the characteristic Zeeman splitting disappears.

The effect of the size of haematite crystallites on Morin temperature (at which a change in orientation of atom spins with respect to the crystallographic axes occurs) was studied with the aid of Mössbauer spectroscopy by Kündig *et al.* (1966). Knowing exactly the average particle size of the analysed haematite samples, those authors have found that Zeeman splitting of *a* —  $\text{Fe}_2\text{O}_3$  observed at room temperature for bulk material disappears for the particle size less than 135 Å, and only a doublet of the quadrupole splitting corresponding to the superparamagnetic state of *a* —  $\text{Fe}_2\text{O}_3$  can be seen.

In their subsequent paper, Kündig *et al.* (1967) have reported that the smaller the haematite particle size, the larger the quadrupole splitting value. The particle size, on the other hand, has very little effect on the isomer shift, which is almost the same as for bulk material.

The values of  $\delta$  and  $2\epsilon$  obtained within the experimental error limits by the present authors for *c* doublet indicate that it corresponds to haema-

tite of medium particle size ( $\leq 70$  Å). It cannot be excluded, however, that a part of  $\text{Fe}^{3+}$  ions corresponding to *c* doublet appear in the form of  $\text{Fe}(\text{OH})_3$ , for which the known isomer shift  $\delta$  (Mathalone *et al.* 1970) has practically the same value whereas the value for the quadrupole splitting,  $2\epsilon = 0.65 \text{ mm}\cdot\text{s}^{-1}$ , is only slightly lower than that obtained for *c* doublet.

The isomer shift  $\delta$  measured for *b* doublet indicates that it is given by goethite, which has been thoroughly investigated in bulk form by several authors. Depending on the origin of samples, simple or composite Zeeman splitting was obtained by Mössbauer spectroscopy at room temperature. Those differences were attributed to the various degrees of goethite hydration. In contrast to the considerable body of knowledge about bulk goethite, the properties of its fine-dispersive forms are less known. The effect of the particle size of *a* —  $\text{FeOOH}$  on the shape of Mössbauer spectra was studied by Shinjo (1966) and van der Kraan *et al.* (1966), who reported only that the Zeeman splitting disappeared at room temperature for the medium goethite particle size below 100 Å. This observation indicates that in the sediments studied here, goethite appears in the form of crystallites of the average size below the cited value.

The doublet *a* corresponds to a compound in which bivalent iron,  $\text{Fe}^{2+}$ , is present while its isomer shift  $\delta$  implies that it is  $\text{FeCO}_3$  (siderite). Siderite is a paramagnetic substance at room temperature. Its Mössbauer spectrum measured by Ono and Ito (1964) shows a single doublet of the quadrupole splitting with the Mössbauer parameters agreeing, within the experimental error limits, with those obtained for *a* doublet.

Mössbauer spectroscopy fails to determine the degree of hydration of goethite or haematite occurring in fine-dispersive forms. Evidence suggesting that form of their occurrence has been provided by chemical analyses and other phase investigations.

## DISCUSSION

The sediments encrusting water intakes may be regarded as ferruginous on the ground of the marked predominance of  $\text{Fe}^{2+}$  and  $\text{Fe}^{3+}$  compounds. The investigations have shown that the body of sediments consists of hydrated fine-dispersive phases, *a* —  $\text{Fe}_2\text{O}_3$  and *a* —  $\text{FeOOH}$ . Moreover, the presence of well-crystallized goethite has been ascertained. The results of X-ray, electron microscope and Mössbauer studies imply that goethite appears in the form of very fine, markedly elongated grains. Also the size of haematite crystallites defined by Mössbauer spectroscopy is suggestive of a high degree of dispersion of that mineral. Another component of the sediments studied is siderite.

Non-iron compounds in the well-encrusting sediments are represented by calcite, amorphous  $\text{SiO}_2$  and  $\text{Al}_2\text{O}_3$  compounds and organic substance. Small concentrations of other components such as  $\text{MgO}$ ,  $\text{MnO}$ ,  $\text{K}_2\text{O}$ ,  $\text{Na}_2\text{O}$ ,  $\text{SO}_3$ , detected by chemical analyses, suggest that their compounds do not appear in the sediments in any significant amounts.

The analyses were also to determine the content of iron mineral phases in the sediments. From chemical analyses and recalculations of the TG curve it appears that goethite makes up 27 — 29 wt. % of all the Fe compounds present in the sediments (Tab. 4) whereas hydrated iron oxides and

Table 4

Quantitative amount of iron compounds in composition of incrustations well obtained as a result of use of different investigations (weight %)

| Phase  | Method of investigation |                         |                  |
|--|-------------------------|-------------------------|------------------|
|  | Chemical analysis       | Thermogravimetric curve | Mössbauer effect |
| $\alpha - \text{FeOOH}$                                    | 27                      | 29                      |                  |
| hydrated oxides and hydroooxides of Fe                     |                         |                         | 46 ± 4           |
| $\alpha - \text{FeOOH} \cdot n\text{H}_2\text{O}$          | 65                      | 59                      | 44 ± 4           |
| $\alpha - \text{Fe}_2\text{O}_3 \cdot n\text{H}_2\text{O}$ |                         |                         |                  |
| $\text{FeCO}_3$  | 8                       | 12                      | 10 ± 4           |

hydroxides constitute together 59 — 65 wt. %. The investigations failed to show, however, how much of that total corresponds to hydrated  $\alpha - \text{FeOOH}$  and how much to hydrated  $\alpha - \text{Fe}_2\text{O}_3$ . This is due, among other reasons, to the fact that the authors give different amounts of water that may be combined during hydration of those iron oxide phases (Minieraly 1967; Krause 1956).

Mössbauer spectroscopy yielded further data permitting to define more accurately the quantitative composition of the sediments (assuming the same value of Debye-Waller factors). The recalculated content of iron compounds making up the well-encrusting sediments is as given in Table 5.

Analyses of Mössbauer spectra taken for the other samples have shown that the nature of the constituent iron oxides and hydroxides is the same. On the other hand in the surface area S corresponding to the individual doublets the Mössbauer spectra indicate that the percentage of siderite is variable, depending on the sampling site.

The above results throw some light on the genesis of the sediments studied. Mössbauer studies do not rule out a possibility that  $\text{Fe}^{3+}$  cations appear partly in the sediment as amorphous  $\text{Fe}(\text{OH})_3$ . This presumption is consistent with the results of earlier investigations of the genesis of sediments of that kind (Krause 1956, 1960). Furtheron, the present studies have revealed that the composition of the sediments in question is strikingly similar to that of the substances obtained by Domka (1975) and Przyłuski (1967) in the course of their investigations aiming to explain the mechanism of goethite crystallization from synthetic  $\text{Fe}(\text{OH})_3$ . It may be presumed that this gel hydroxide is the primary substance in the incrustations.

Table 5  
Content of iron mineral in incrustations well (weight %)

| Phase  | Content    |
|--|------------|
| $\alpha - \text{FeOOH}$                                    | 27—29      |
| $\alpha - \text{FeOOH} \cdot n\text{H}_2\text{O}$          | ca. 18 ± 4 |
| $\alpha - \text{Fe}_2\text{O}_3 \cdot n\text{H}_2\text{O}$ | 44 ± 4     |
| $\text{FeCO}_3$  | 8—12       |

station processes, which by aging and crystallization, controlled by the pH and Eh of the environment, passes into the liquid oxide phase and then into goethite. A solution of that problem, as well as a precise determination of the content of iron compounds in the sediments would require appropriate Mössbauer measurements to be carried out on model samples. In the present case, the whole issue is additionally confused by the lack of data concerning the effect of the shape and size of iron mineral crystallites on Debye temperature of those compounds.

## REFERENCES

- [ALEKSEJEW W. S.] АЛЕКСЕЕВ В. С., 1975: Биологический кольматаж скважин. Гидротехника и Мел. № 4.
- BARNES I., CLARKE F. E., 1969: Chemical properties of ground water and their corrosion and encrustation effects on wells. *Geol. Surv. Professional Paper* 498-D.
- BUETELSPAHER H., VAN DER MAREL H. M., 1968: Atlas of electron microscopy of clay minerals and their admixtures. Elsevier Publishing Comp. Amsterdam—London—New York.
- DOMKA F., 1975: Właściwości fizyko-chemiczne i katalityczne produktów temperaturowych przemian wodorotlenków i tlenowodorotlenków żelaza. UAM seria Chemia nr 17.
- GARRELS P. M., CHRIST C. L., 1965: Solutions, minerals-equilibria. New York.
- [GAWRIŁKO W. M.] ГАВРИЛКО В. М., 1968: Фильтры водозаборных, водопонизительных, гидрологических скважин. Москва.
- HEM J. D., 1970: Study and interpretation of the chemical characteristic of natural water. *Geol. Surv. Water — Supply Paper* vol. 1473.
- KRAUSE A., 1956: O ferromagnetycznych związkach tlenków metali i nowej metodzie ich otrzymywania. *Przem. Chemiczny* rocz. XII (35) nr 11.
- KRAUSE A., 1960: O katalizatorach heterogennych i mechanizmie reakcji katalitycznych. *Nauka Polska* rok VIII nr 4(32).
- KUNDIG W., BOMEL H., CONSTABARIS G., LINDQUIST R. H., 1966: Some properties of supported small  $\alpha - \text{Fe}_2\text{O}_3$  particles determined with the Mössbauer effect. *Phys. Rev.* 142, 327.
- KUNDIG W., ANDO K. J., LINDQUIST R. H., CONSTABARIS G., 1967: Mössbauer study of ultrafine particles of  $\text{NiO}$  and  $\alpha - \text{Fe}_2\text{O}_3$ . *Czechosl. J. Phys.* B17, 467.
- [КОММУНАР Г. М.] КОММУНАР Г. М., 1974: Исследование процессов химического кольматажа скважин и разработка методики прогноза снижения их производительности. ВНИИ „Водгро“ Москва.
- MARTON L., SELLYEY G., 1971: Eltömödött vizadé kutek feltra sának tapasztalatei. *Hidrol. Közlöny* No 3.
- MATHALONE Z., RON M., BIRAN A., 1970: Magnetic ordering in iron gel. *Sol. State Comm.* 8, 333.
- [МИЛИХИКЕР А. Т.] МИЛИХИКЕР А. Т., 1971: Осадкообразование в скважинах водоизмещения. Москва.
- [МИНЕРАЛЫ] МИНЕРАЛЫ 1967. АН СССР т. II вып. 3. Москва.
- ONO K., ITO A., 1964: Mössbauer study of magnetic properties in ferrous compounds. *J. Phys. Soc. Japan* 19, 899.
- PRZYŁUSKI J., 1967: Otrzymywanie tlenków żelaza metodą elektrochemiczną. *Zeszyt Naukowe Polit. Warszawskiej* nr 158. Chemia zeszyt 6.
- RATAJCZAK T., WITCZAK S., 1973: Mineralogia i geochemia osadów żelazistych tworzących się w ujściach wód podziemnych rejonu Włocławka. *Prace Mineralogiczne* 40.
- RATAJCZAK T., 1976: Zastosowanie spektrofotometrii absorpcyjnej w podczerwieni do badania substancji organicznej osadów kolmatujących studnie. *Spraw. z Pos. Kom. Nauk. Mineral. Styczeń—czerwiec.*
- SHINJO T., 1966: Mössbauer effects in antiferromagnetic fine particles. *J. Phys. Japan* 21, 917.

- The X-ray identification and crystal structures of clay minerals. (Ed. by G. Brown). London 1961.
- [TIURIN I. W.] ТИУРИН И. В., 1951: К методике для сравнительного изучения состава почвенного гумуса. Труды Почв. НС СССР т. 8.
- VAN DER KRAAN A. M., VAN LOEF J. J., 1966: Superparamagnetism in submicroscopic  $\alpha$ -FeOOH particles observed by the Mössbauer effect. *Phys. Lett.* 20, 614.
- WHITE W. B., ROY R., 1964: Infra-red spectra — crystal structure correlations. II. Comparissoin of simple polymorphic minerals. *Am. Mineral.* vol. 49 No 11—12.

Tadeusz RATAJCZAK, Stanisław WITCZAK, Dominik S. KULGAW-CZUK, Janusz KRACZKA

## BADANIA CHARAKTERU POŁĄCZEŃ ŻELAZA W OSADACH KOLMATUJĄCYCH STUDNIE

### Streszczenie

Celem pracy było zanalizowanie składu mineralnego osadów wytrącających się w studniach. Szczególną uwagę poświęcono wyjaśnieniu charakteru i struktury tworzących je minerałów żelaza. Przedmiotem badań była uśredniona próbka osadów kolmatujących filtr, pobrana z ujęcia wodnego na terenie miasta Krakowa. Dla określenia składu fazowego osadów wykonano analizę chemiczną, termiczną, rentgenograficzną i spektroskopową w podczerwieni. Przeprowadzone badania z zastosowaniem transmisyjnego mikroskopu elektronowego służyły określeniu wielkości ziarn tlenków żelaza, jak również ustaleniu ich cech strukturalnych i teksturalnych. Wielkość krystalitów określano za pomocą wzoru P. Scherrera. Podobnego rodzaju wiadomości miała dostarczyć także metoda spektroskopii móssbauerowskiej.

Analizy chemiczne wykazały, że podstawowym składnikiem badanych osadów jest  $Fe_2O_3$ , a następnie  $CaO$  i  $FeO$ . Podróżnie występują  $SiO_2$  i  $Al_2O_3$ . Duża zawartość tlenków żelaza ( $Fe_2O_3 + FeO = 64,05\%$  wag.) upoważnia do określenia ich jako osady żelaziste. Podstawową treść osadów kolmatujących studnie stanowią uwodnione tlenki żelaza: hydrohematyty i hydrogetyty oraz wodorotlenki — getyty. Intensywność refleksów otrzymanych na krzywych dyfraktometrycznych przemawia za tym, że w największej ilości występują tlenki uwodnione — hydrogetyt i hydrohematyty. Kształt refleksów sugeruje poza tym, że w przypadku badanych osadów mamy do czynienia z nagromadzeniami drobnodispersyjnymi tlenkowych faz mineralnych żelaza, o niewysokim stopniu uporządkowania budowy wewnętrznej, względnie z zakłóceniemi w strukturze. Analiza dyfraktometryczna wykazała także obecność węglanów: kalcytu i syderytu.

Dominującymi organiami występującymi na krzywych spektralnych w podczerwieni są organia pochodzące od tlenków i wodorotlenków żelaza. Należą do nich m.in. intensywne organia metalotlenowe. Znaczny stopień

uwodnienia tych połączeń jest potwierdzony drganiami deformacyjnymi i walencyjnymi pochodząymi od drobin wody.

Na krzywej TG zaznaczają się dwa wyraźne zakresy ubytku masy badanej substancji. Pierwszy z nich (100—400°C) wynika ze straty wody zawartej w uwodnionych tlenkach i wodorotlenkach żelaza oraz z rozkładu substancji organicznej i siarczków. Drugi (500—800°C) wywołany jest rozkładem węglanów.

Przegląd preparatów elektronowych wykazał, że poszczególne ziarna wykazują nieregularne kształty. Porównując otrzymane zdjęcia ze wzorcowymi stwierdzono ich wyraźne podobieństwo do getytu oraz tlenków żelaza. Wielkość poszczególnych ziarn jest rzędu 100—500 Å.

Wyznaczono wymiary krystalitów getytu. Otrzymano następujące wyniki:  $\perp$  do (110) — 39,14 Å,  $\perp$  do (010) — 19,04 Å.

Uzyskane przy pomocy metody spektroskopii móssbauerowskiej wartości przesunięcia izomerycznego  $\delta$  i rozszczepienia kwadrupolowego  $2\epsilon$  dubletu (symbol  $a$  na fig. 5) są typowe dla związków, w których żelazo występuje w stanie wysokospinowym  $Fe^{2+}$ , natomiast wartości te dla dubletów oznaczonych  $b$  i  $c$  wskazują na związki, w których żelazo występuje w stanach wysokospinowych  $Fe^{3+}$ . Wartości  $\delta$  i  $2\epsilon$  z pomiarów dla dubletu  $c$  wskazują, że odpowiadają one hydrohematytyowi o średnich wymiarach częstek około 70 Å. Nie można jednak wykluczyć, że część jonów  $Fe^{3+}$  odpowiadająca dubletowi  $c$  występuje w postaci  $Fe(OH)_3$ . Wartości zmierzone dla dubletu  $b$  wskazują, że pochodzi on od getytu. Minerał ten występuje w formie częstek o wielkości poniżej 100 Å. Dublet  $a$  odpowiada związkowi, w którym żelazo występuje w postaci  $Fe^{2+}$ , a jego  $\delta$  wskazuje że jest nim  $FeCO_3$ .

Badania fazowe pozwoliły na ustalenie składu ilościowego w zakresie połączeń żelaza (w przeliczeniu na 100%). Przedstawia się on następująco:  $a - FeOOH$  27—29,  $a - FeOOH \cdot nH_2O$  około 18,  $a - Fe_2O_3 \cdot nH_2O$  — 44,  $FeCO_3$  — 8—12 (w % wag.).

Rezultaty badań z zastosowaniem efektu Mössbauera nie wykluczają faktu, że część kationów  $Fe^{3+}$  może występować w osadzie w postaci żelazowego  $Fe(OH)_3$ . Można przypuszczać, że stanowi on substancję pierwotną w procesie kolmatacji, która drogą starzenia się i krystalizacji uwarunkowanych wartościami pH i Eh środowiska przechodzi w fazę uwodnionych tlenków żelaza, a następnie w getyt.

### OBJAŚNIENIA FIGUR

Fig. 1. Krzywa dyfraktometryczna osadów żelazistych kolmatujących studnie:  $G$  — getyt,  $hG$  — hydrogetyt,  $H$  — hematyt,  $hH$  — hydrohematyty,  $C$  — kalcyt,  $S$  — syderyty.

Fig. 2. Spektrogram absorpcyjny w podczerwieni osadów wytrącających się w ujęciach wodnych  
 $G$  — getyt

Fig. 3. Krzywa termograwimetryczna badanych osadów  
 $I$  — straty wagowe powstałe w wyniku uwodnienia uwodnionych tlenków i wodorotlenków Fe, rozkładu pirytu i spalania substancji organicznej,  $II$  — straty wagowe powstałe w wyniku rozkładu syderytu

Fig. 4. Kryształ getytu (wg Goldschmidta i Parsons 1910) z naniesionymi wartościami jego parametrów

Fig. 5. Widmo mōssbauerowskie osadów żelazistych wykonane w temperaturze pokojowej

2ε — rozszczepienie kwadrupolowe, (a, b, c) — położenia poszczególnych dubletów rozszczepień kwadrupolowych

#### OBJAŚNIENIA FOTOGRAFII

- Fot. 1. Skupienia ziarn tlenków żelaza o nieregularnych kształtach. Pow. × 48 000  
Fot. 2. Nagromadzenie tlenków żelaza o budowie ziarnistej z wyraźnie rozwiniętą linią brzegową. Pow. × 30 000  
Fot. 3. Ziarna tlenków żelaza o trójkątnych zarysach i ostrych konturach. Pow. × 80 000  
Fot. 4. Cząstki badanego osadu o budowie blaszkowej tworzące agregaty. Pow. × 100 000  
Fot. 5. Blaszki mineralów tlenkowych żelaza z nieregularnymi „karbowanymi” krawędziami. Pow. × 80 000

#### OBJAŚNIENIA TABEL

- Tab. 1. Skład chemiczny badanych osadów  
Tab. 2. Przybliżony skład fazowy badanego osadu otrzymany w efekcie przeliczeń analizy chemicznej i krzywej ubytku masy  
Tab. 3. Zestawienie wartości rozszczepień kwadrupolowych  $2\epsilon$ , przesunięć izomerycznych  $\delta$  i procentowych wielkości powierzchni  $S$  dla poszczególnych dubletów (a, b, c)  
Tab. 4. Ilościowy udział mineralów żelaza w składzie osadów kolmatujących studnie otrzymany w rezultacie zastosowania różnych metod badawczych (w przeliczeniu na 100%)  
Tab. 5. Zawartość mineralów żelaza w osadach kolmatujących studnie (w przeliczeniu na 100%)

Тадеуш РАТАЙЧАК, Станислав ВИТЧАК, Доминик С. КУЛЬГАВЧУК,  
Януш КРАЧКА

### ИССЛЕДОВАНИЕ ХАРАКТЕРА СВЯЗЕЙ ЖЕЛЕЗА В ОСАДКАХ КОЛЬМАТИРУЮЩИХ КОЛОДЦЫ

#### Резюме

Целью работы являлся анализ минерального состава наносов осаждающихся в колодцах. Особенное внимание уделено выяснению характера и структуры слагающих их минералов железа. Предметом исследования являлся средний образец осадков кольматирующих фильтр, отобранный из водозабора на территории города Krakowa. С целью определения фазового состава осадков проведены химический, термический, рентгенографический и ИК-спектроскопический анализы. Исследования, проведенные с применением трансмиссионного электронного микроскопа, послужили для

определения размеровзерен окислов железа, а также для определения их структурных и текстурных свойств. Размеры кристаллитов определено по формуле П. Шеррера. Подобного рода информацию должен дать и метод мёссбауэрowej спектроскопии.

Химические анализы показали, что основным компонентом изучаемых осадков является  $Fe_2O_3$ , а потом  $CaO$  и  $FeO$ . Подчиненное значение имеют  $SiO_2$  и  $Al_2O_3$ . Большое содержание окислов железа ( $Fe_2O_3 + FeO = 64,05\%$ ) дает возможность назвать их железистыми осадками. В кольматирующих колодцах осадках в основном содержатся гидраты окислов железа: гидрогематит и гидрогетит; гидроокислы — гетит. Кроме того, форма рефлексов указывает, что в случае исследуемых осадков имеет дело с мелкодисперсными скоплениями окисных минеральных фаз железа о невысокой степени упорядоченности, или с дефектами структуры. Рентгеновский анализ обнаружил также присутствие карбонатов: кальцита и сидерита.

Преобладающими полосами на ИК-спектрах являются полосы поглощения окислов и гидроокислов железа. К ним принадлежат интенсивные полосы металлокислых колебаний. Значительная степень гидратации этих связей подтверждается дефор-полосами поглощения молекулы воды.

На кривой TG обозначаются два четких интервала потери веса изучаемого вещества. Первый из них (100—400°C) вызван водой, содержащейся в гидратированных окислах и гидроокислах, а также органическим веществом и сульфидами. Второй (500—800°C) связан с разложением карбонатов.

Просмотр электронных изображений показал, что отдельные зерна характеризуются неправильными формами. Сравнивая полученные изображения с эталонными, обнаружено их явное сходство с гетитом и окислами железа. Большинство отдельных зерен порядка 100—500 Å.

Определено размеры кристаллитов гетита. Получено следующие результаты:  $\perp$  k (110) — 39,14 Å,  $\perp$  k (010) — 19,04 Å.

Значения изомерного смешения  $\delta$  и квадрупольного расщепления дуплета  $2\epsilon$  (символ  $a$  на фиг. 5), полученные методом мёссбауэрowskoy спектroskopii, типичны для соединений, в которых железо находится в высокоспинном состоянии  $Fe^{3+}$ . Значение  $\delta$  и  $2\epsilon$  измерений для дуплета  $c$  указывают, что они соответствуют гидрогематиту о средних размерах частиц порядка 70 Å. Однако не можно исключить, что часть ионов  $Fe^{3+}$ , соответствующая дуплету  $c$ , находится в виде  $Fe(OH)_3$ . Полученные для дуплета  $b$  значения указывают, что он происходит от гетита. Этот минерал встречается в форме частиц размером меньше 100 Å. Дуплет  $a$  соответствует соединению, в котором железо находится в виде  $Fe^{2+}$ , а его  $\delta$  указывает, что это  $FeCO_3$ .

Фазовые исследования позволили установить количественный состав соединений железа (в пересчете на 100%). Он представляется следующим образом:  $a$  —  $FeOOH$  — 27—29,  $a$  —  $FeOOH \cdot nH_2O$  около 18,  $a$  —  $Fe_2O_3 \cdot nH_2O$  — 42,  $FeCO_3$  — 8—12 (в вес. %).

Результаты исследования с применением эффекта Мёссбауэра не исключают факта, что часть катионов  $Fe^{3+}$  может присутствовать в осадке в виде геля  $Fe(OH)_3$ . Можно полагать, что он является первичным веществом в процессе кольматажа, которое путем старения и кристаллизации, обусловленной значениями pH и Eh среды, переходит в фазу гидратированных окислов железа, а затем в гетит.

## ОБЪЯСНЕНИЯ К ФИГУРАМ

- Фиг. 1. Дифрактограмма кольматирующих колодцы железистых осадков  
 G — гетит,  $hG$  — гидрогетит, H — гематит,  $hH$  — гидрохематит, C — кальцит, S — сидерит
- Фиг. 2. ИК-спектр наносов осаждающихся в водозаборах  
 G — гетит
- Фиг. 3. Термогравиметрическая кривая исследуемых осадков  
 I — потери веса вследствие дегидратации гидратных окислов и гидроокислов железа, разложение пирита и горения органического вещества, II — потери веса вследствие разложения сидерита
- Фиг. 4. Кристалл гетита (по Гольдшмидту и Парсонсу, 1910) с нанесенными значениями его параметров
- Фиг. 5. Мессбауэровский спектр железистых осадков фиксированный в комнатной температуре  
 $2\varepsilon$  — квадрупольное расщепление, (a, b, c) положения отдельных дуплетов квадрупольных расщеплений

## ОБЪЯСНЕНИЯ К ФОТОГРАФИЯМ

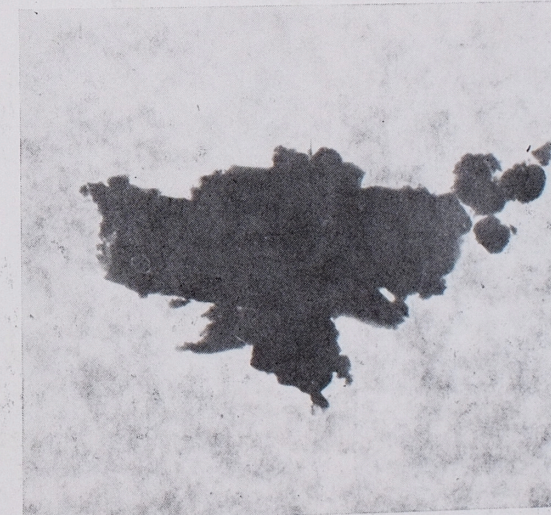
- Фот. 1. Скопления зерен окислов железа неправильных форм.  $\times 48\ 000$
- Фот. 2. Нагромождение окислов железа зернистой структуры с отчетливо развитой краевой линией.  $\times 30\ 000$
- Фот. 3. Зерна окислов железа треугольных форм и четких контуров.  $\times 80\ 000$
- Фот. 4. Агрегаты частиц изучаемого осадка пластинчатого строения.  $\times 100\ 000$
- Фот. 5. Пластины окисных минералов железа с „рифлёнными” краями.  $\times 80\ 000$

## СПИСОК ТАБЛИЦ

- Табл. 1. Химический состав исследуемых осадков
- Табл. 2. Приближенный фазовый состав исследуемого осадка, полученный в итоге пересчета химического анализа и кривой потери веса
- Табл. 3. Сопоставление значений квадрупольных расщеплений  $2\varepsilon$ , изомерных смещений  $\delta$  и процентной величины площади  $S$  отдельных дуплетов (a, b, c)
- Табл. 4. Количественное соотношение железистых минералов в составе кольматирующих колодцы осадков, полученное в итоге применения различных исследовательских методов (в пересчете на 100%)
- Табл. 5. Содержание железистых минералов в осадках кольматирующих колодцы (в пересчете на 100%)



Phot. 1. Aggregate of grains of iron oxides with irregular shapes.  
 $\times 48\ 000$



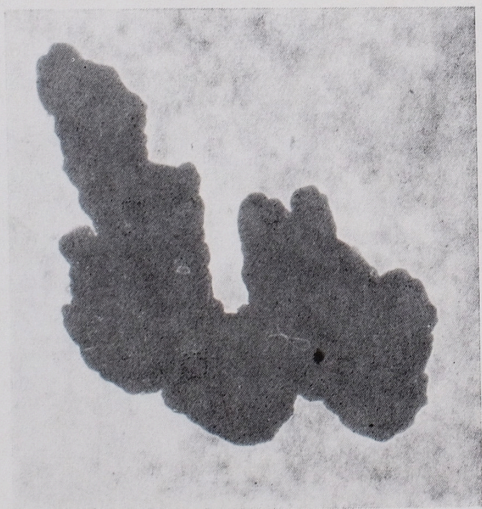
Phot. 2. Accumulation of oxide iron forms with distinct sharp-bordered borders.  $\times 30\ 000$



Phot. 3. Grains of iron oxides with sharp lines and visible triangular angles.  $\times 80\,000$



Phot. 4. Particles of incrustation formed from grains with flaky structure.  $\times 100\,000$



Phot. 5. Plates of iron oxides with irregular outlines.  $\times 80\,000$